

# Measurements of the quantum-confined conduction band energy in the wetting layer surrounding individual $\text{In}_{0.4}\text{Ga}_{0.6}\text{As}$ quantum dots by cross-sectional ballistic electron emission microscopy

C. Marginean and J. P. Pelz

*Department of Physics, The Ohio State University, Columbus, Ohio 43210-1106, USA*

S. Y. Lehman

*Department of Physics, The College of Wooster, Wooster, Ohio 44691, USA*

J. G. Cederberg

*Sandia National Laboratories, Albuquerque, New Mexico 87123, USA*

(Received 2 November 2009; revised manuscript received 30 April 2010; published 12 July 2010)

We measured the quantum-confined conduction band minimum (CBM) energy in the wetting layer (WL) around and behind cleaved self-assembled  $\text{In}_{0.4}\text{Ga}_{0.6}\text{As}$  quantum dots (QDs) using cross-sectional ballistic electron emission microscopy (XBEEM) at room temperature. With the probe tip positioned over a QD, the dependence of the measured CBM energy on the reverse bias confirmed that XBEEM measured the CBM energy in the *wetting layer at the backside* of the QD and not in the QD itself. Measurements indicated that the CBM of the quantum-confined wetting layer is approximately 90 meV below the GaAs CBM, and that this conduction band offset is not substantially affected by pinning effects at the metal/semiconductor interface. The amplitude of the BEEM current entering a WL was also observed to *decrease* once the deposited thickness of an  $\text{In}_{0.4}\text{Ga}_{0.6}\text{As}$  or InAs layer exceeded a certain threshold, consistent with a reduction in the WL thickness after large-scale QD formation takes place.

DOI: [10.1103/PhysRevB.82.035304](https://doi.org/10.1103/PhysRevB.82.035304)

PACS number(s): 73.30.+y, 73.63.Kv

## I. INTRODUCTION

Quantum dots (QDs) are under active investigation for applications ranging from laser diodes to single-photon sources<sup>1-4</sup> and have also been proposed as good candidates for nanodevices especially in the developing field of the quantum information processing.<sup>5-7</sup> Quantum dots also provide an excellent system to study the fundamental physical properties of systems exhibiting carrier confinement in zero dimensions.<sup>8</sup> For QDs formed during strained-layer growth via the Stranski-Krastanow growth mode, a two-dimensional (2D) “wetting layer” (WL) initially forms, and subsequently evolves into three-dimensional islands, producing the quantum dots.<sup>9</sup> However, an extended WL remains after the QDs have formed that should behave as a laterally inhomogeneous 2D quantum well (QW) and should affect the electronic properties of the embedded QDs. Since optical spectroscopy measurements have confirmed that the WL indeed affects the electronic properties of the self-assembled QDs,<sup>10-13</sup> it is important to characterize the electronic properties of the (inhomogeneous) WL itself with high spatial resolution.

In this paper we report the electronic measurements of the position-dependent conduction band minimum (CBM) energy of the WL (both at the metal/WL interface and at the QD/WL interface at the *back side* of cleaved  $\text{In}_{0.4}\text{Ga}_{0.6}\text{As}$  QDs) and the CBM of the surrounding metal/GaAs host interface, using cross-sectional ballistic electron emission microscopy (XBEEM) on a Schottky contact made to a cleaved QD sample. By applying a reverse bias to the Schottky contact and measuring the resulting effect on the measured local Schottky barrier height (SBH), we can distinguish the *depth* at which the “high point” occurs in the CB profile beneath

the probe tip, and we find that when the probe tip is located over a cleaved QD this high point occurs at the backside of the  $\text{In}_{0.4}\text{Ga}_{0.6}\text{As}$  QD. A comparison of these measurements indicates that conduction band offset between the GaAs host and the quantum-confined wetting layer is  $\sim 90$  meV, and that this offset is not substantially modified by Fermi-level pinning effects at the metal/semiconductor interface. We also observed that an applied reverse bias strongly increases transmission through most of the measured QDs but does not substantially affect hot-electron transmission through the surrounding metal/GaAs interface.

## II. EXPERIMENT

The sample analyzed was grown by metal-organic vapor phase epitaxy and consisted of a sequence of three  $\text{In}_{0.4}\text{Ga}_{0.6}\text{As}$  QD layers and four InAs QD layers as indicated in Table I. The details of QD growth have been reported previously.<sup>13,14</sup> For this specific structure each QD layer was embedded in GaAs by growing a 50-nm-thick layer (doped at  $5 \times 10^{16}/\text{cm}^3$  *n* type) on each side of the QD layer. The capping layer eliminates the strain field of the underlying QDs, limiting their impact on subsequent QD layers.<sup>15</sup> Adjacent QD/GaAs structures were separated by marker layer of  $\text{Al}_{0.3}\text{Ga}_{0.7}\text{As}$  ( $1 \times 10^{17}/\text{cm}^3$  *n*-type doping) of thickness varying from 80 nm (closest to the GaAs substrate) to 30 nm (closest to the top capping layer). The variable  $\text{Al}_{0.3}\text{Ga}_{0.7}\text{As}$  thickness allows us to unambiguously identify each QD layer in the BEEM images. This sequence of layers was grown on a 500 nm GaAs buffer layer ( $2 \times 10^{15}/\text{cm}^3$  *n* type) grown on a GaAs substrate ( $2 \times 10^{17}/\text{cm}^3$  *n* type) and was capped with a 1500 nm top GaAs layer ( $5 \times 10^{16}/\text{cm}^3$  *n* type).

TABLE I. Deposition thicknesses of the QD layers. Layer numbering starts from the buffer layer toward the cap layer.

Layer No.	Material	Thickness (nm)
1	In <sub>0.4</sub> Ga <sub>0.6</sub> As	1.56
2	In <sub>0.4</sub> Ga <sub>0.6</sub> As	2.04
3	In <sub>0.4</sub> Ga <sub>0.6</sub> As	3.00
4	InAs	0.297
5	InAs	0.656
6	InAs	0.595
7	InAs	0.543

In order to make the XBEEM measurements, the sample was prepared in a similar way as previously described for XBEEM measurements of AlGaAs/GaAs quantum well samples.<sup>16</sup> It was cleaved *ex situ* and quickly inserted into a deposition chamber and pumped to  $2 \times 10^{-7}$  torr, and a 7-nm-thick Au film was thermally evaporated through a shadow mask to form 300  $\mu\text{m}$  diameter Schottky barrier contacts. Figure 1 shows a side view schematic of the resulting sample. The sample was then introduced in a modified UHV Omicron variable temperature scanning tunneling microscope (STM). Room-temperature BEEM was used to locate and image the subsurface QDs and the adjacent layers in a manner similar to that discussed in Ref. 16.

In BEEM, the hot electrons are injected into the Au metal film using the STM tip which is held at bias  $-V_T$  (tip voltage) with respect to the metal film. If the Au film is sufficiently thin, the injected hot electrons having energies equal or larger than local Schottky barrier height can reach and surmount the barrier in order to enter the conduction band of the semiconductor. These electrons are collected as a BEEM collector current  $I_C$ . By positioning the tip at a certain location and measuring a BEEM  $I_C$ - $V_T$  curve (also known as a BEEM spectrum) the local SBH can be determined as  $\phi_{\text{SB}} = eV_{\text{TH}}$ , where  $V_{\text{TH}}$  is the BEEM threshold voltage for observing  $I_C$ , and  $e$  is the elementary charge. The Bell-Kaiser (BK) model<sup>17</sup> with a one threshold fit for the BEEM  $I_C$ - $V_T$  curves was used to determine  $V_{\text{TH}}$ .

### III. RESULTS AND DISCUSSION

Figure 2(a) shows a  $1 \mu\text{m} \times 1 \mu\text{m}$  area BEEM image of

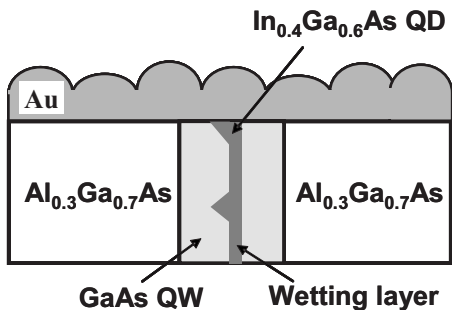


FIG. 1. Schematic diagram (not to scale) of one cleaved QW/QD layer surrounded by AlGaAs layers.

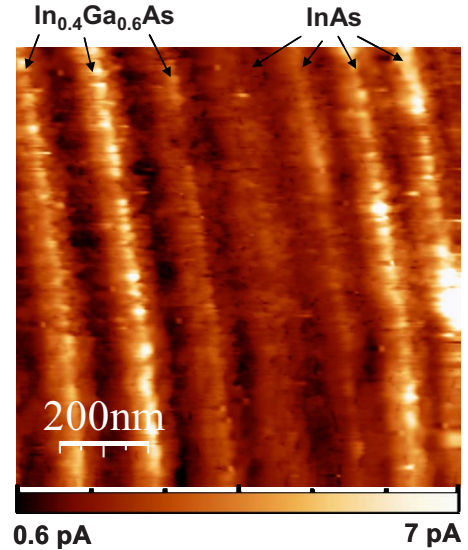


FIG. 2. (Color online) BEEM image of the seven GaAs QD layers listed in Table I, recorded with tunnel current  $I_T = 20$  nA and tip voltage  $V_T = 1.1$  V. Layer No. 1 in Table I corresponds to the leftmost layer observed in the image. The brightest, intermediate, and dimmest parts of each layer correspond to the InGaAs (or InAs), GaAs, and AlGaAs regions, respectively.

the metal/cleaved QD interface, showing all seven QD layers, with the GaAs substrate to the left and the GaAs capping layer to the right. The GaAs and InGaAs/InAs QD layers have lower local SBH than the AlGaAs layers and so show up as bright regions in BEEM images. Starting from this large area image we can identify and zoom-in on a particular QD layer when acquiring subsequent images. All the detailed QD data in the rest of this paper were measured over QD layer No. 2 from Table I, corresponding to the second bright layer from the left in Fig. 2.

In order to locate particular QDs, we measured a closeup BEEM image of the metal/cleaved QD interface, as shown in Figs. 3(b) and 3(c). The tip was held at  $V_T = 1.15$  V when it was scanned from left-to-right (LtoR) for Figs. 3(a) and 3(b) but was held at  $V_T = 0.80$  V when it was scanned from right-to-left (RtoL) for Fig. 3(c). All images were recorded with a tunnel current  $I_T = 20$  nA. For Fig. 3(b), the tip voltage  $V_T = 1.15$  V is larger than the SBH for all parts of this sample so BEEM current is observed everywhere. However, enhanced current is seen over regions with lower SBH, allow-

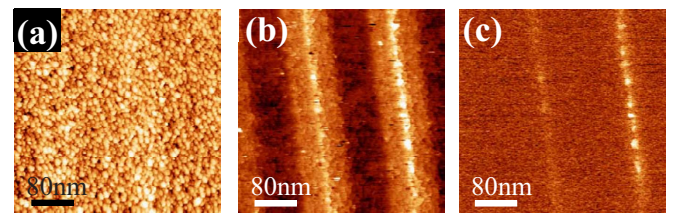


FIG. 3. (Color online) (a) LtoR STM image of the Au top film and (b) simultaneous BEEM image measured with  $V_T = 1.15$  V of a portion of QD layer Nos. 1 and 2, and (c) interleaved right-to-left (RtoL) BEEM image of the same region measured with  $V_T = 0.80$  V.

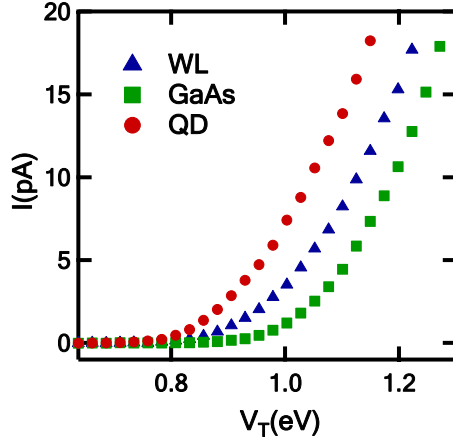


FIG. 4. (Color online) Typical BEEM spectra measured in layer No. 2 with a tunneling current of 20 nA over (from left to right) a QD, the surrounding WL and GaAs with SBHs of 0.787 eV, 0.818 eV, and 0.911 eV respectively.

ing us to easily distinguish the AlGaAs layers (the darkest regions with the smallest BEEM current), the GaAs layers (intermediate current), and the InGaAs QD layer (brightest).

In order to more clearly image the cleaved wetting layer and the InGaAs/InAs QDs, the tip voltage was reduced to  $V_T=0.8$  V in the RtoL BEEM image, as shown in Fig. 3(c). In this case the injected hot electrons were able to surmount the Au/InGaAs SB, but not the SB of Au/GaAs or Au/AlGaAs, which have SBHs of  $\sim 0.90$  eV and  $\sim 1.085$  eV,<sup>16</sup> respectively. This allows us to clearly distinguish individual InGaAs QDs from the surrounding InGaAs wetting layer. After we have identified regions with enhanced BEEM current, we then positioned the tip at specific locations, and measured a set of ten successive BEEM  $I_C-V_T$  curves, which were averaged together (to improve signal-to-noise ratio) and were fit to determine the local SBH. Figure 4 shows typical BEEM spectra measured in layer No. 2 over (from left to right) a QD, the surrounding WL and GaAs regions of the sample, respectively, showing progressively higher SBHs of 0.787 eV, 0.818 eV, and 0.911 eV, respectively.

Figure 5 shows a larger area BEEM image of a different part of this same  $\text{In}_{0.4}\text{Ga}_{0.6}\text{As}$  QD layer, indicating measured local SBHs at different locations along the QD layer. It can be observed in Fig. 5 that regions with enhanced BEEM current tend to have lower SBHs than regions with lower BEEM current. We attribute regions with the lowest SBH to be QDs and other regions along the QD layer to be the remaining WL. We later describe a procedure that uses BEEM to determine the physical depth of particular QDs.

It is important to understand that the measured SBH represents the *highest* energy point in the conduction band profile between the metal interface and the semiconductor bulk, and is in general located at some depth below the physical metal/semiconductor interface. For a uniform metal/semiconductor Schottky contact, this nonzero depth is due to the well-known effect of “image force lowering” (IFL),<sup>18</sup> which causes the high point in the CB profile to be located at a certain depth that is less than 2 nm for typical metal/GaAs Schottky barriers. IFL also causes this high-point energy to

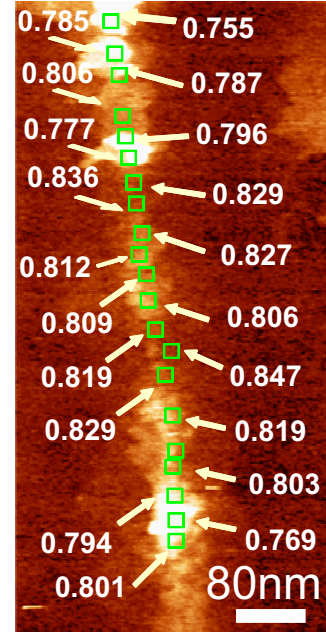


FIG. 5. (Color online) BEEM image of part of layer No. 2, showing locations of local BEEM  $I_C-V_T$  measurements and determined local SBHs.

be lower than the “intrinsic” SBH by an amount  $\Delta\phi_{IF} = \sqrt{qE_d/4\pi\epsilon_s\epsilon_0}$ , where

$$E_d = \frac{qN_D}{\epsilon_0\epsilon_s} \sqrt{\frac{2\epsilon_0\epsilon_r}{qN_D} \left[ \phi_{SB} - \frac{k_B T}{q} \ln\left(\frac{N_C}{N_D}\right) - \frac{k_B T}{q} + V_R \right]} \quad (1)$$

is the depletion electric field near the metal/semiconductor interface,  $N_D$  is the doping concentration,  $\phi_{SB}$  is the intrinsic Schottky barrier height,  $N_C$  is the effective density of states in conduction band,  $V_R$  is the applied reverse bias, and  $\epsilon_s$  is the semiconductor permittivity.<sup>18</sup> For a uniform Au/GaAs interface with  $\phi_{SB} \cong 0.90$  eV and  $N_D \cong 5 \times 10^{16}/\text{cm}^3$  substrate doping, we expect  $\Delta\phi_{IF} \cong 35$  meV for  $V_R=0$  V, with an additional lowering of  $\delta(\Delta\phi_{IF}) \cong 8$  meV if  $V_R$  is increased to 1 V. The IFL effect due to the applied bias is illustrated in Fig. 6(c).

However, if the substrate has *structure* below the metal interface (due, for example, to a buried  $p-n$  junction<sup>19</sup> or epitaxial layers<sup>20</sup>) then the high point in the CB profile can be substantially deeper. This is illustrated in Fig. 6, which assumes that an interface to a different material with a higher CB (by an amount  $\Delta\text{CB}$ ) that exists at a physical depth  $d$  below the metal interface. Figure 6 shows two possible situations. Case A [Fig. 6(a)] assumes that  $d$  is sufficiently large and/or  $\Delta\text{CB}$  is sufficiently small that the high point in the CB still occurs close to the metal interface. In contrast, Case B [Fig. 6(b)] assumes that the high point is located at the physical depth  $d$  with a peak barrier height  $\phi_{back}$  when  $V_R=0$  V, which is equal to the energy of the CBM of the WL at that depth. These two situations will behave differently under an applied reverse bias. In Case A, an applied reverse bias will

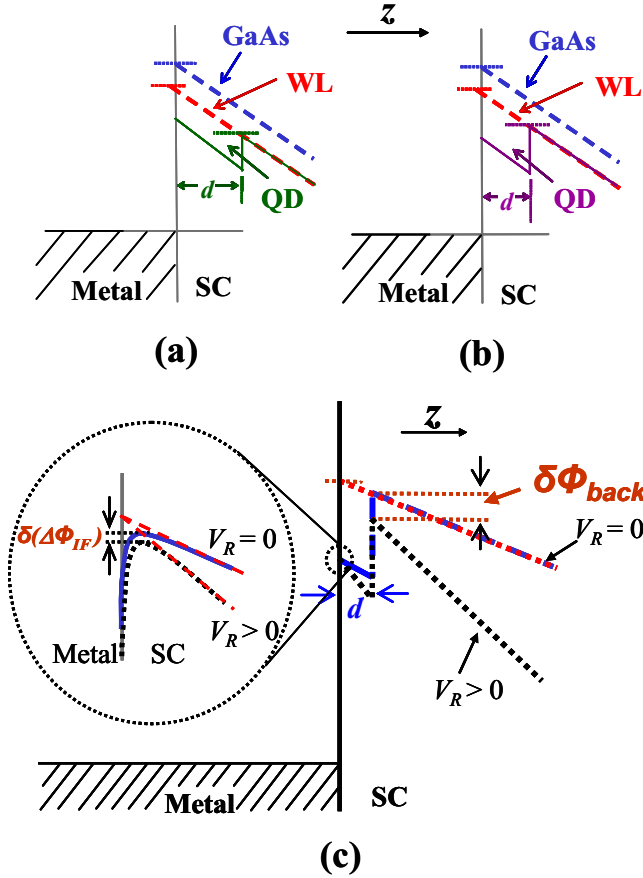


FIG. 6. (Color online) (a) Energy-level diagram with the high point of the SBH at the front side of the quantum dot. (b) Energy-level diagram with the high point of the SBH at the back side of the quantum dot. The energy-level diagram does not include image force lowering at the metal/semiconductor interface. (c) Closeup view illustrating the IFL effect at the front side of the QD and  $\delta\Phi_{back}$  at the back side of the QD due to a reverse bias.

produce only a small additional barrier lowering as discussed above for the case of a uniform Schottky contact. In Case B however, there should be a larger lowering with applied reverse bias [see Fig. 6(c)], by an amount,

$$\delta\phi_{back} \cong d\Delta E, \quad (2)$$

where  $\Delta E$  is the change in the depletion field in the vicinity of the QD.

In this experiment, we first determined whether the SBH measured over specific cleaved QDs falls into Case A or Case B (i.e., whether the high point of the CB profile is at the metal interface or at the backside of the QD) by measuring the change in SBH due to an applied reverse bias. In those cases where we determine that the high point is at the back side of the QD, we then use the measured lowering to estimate the physical depth of a cleaved QD using Eq. (2).

The experiment was conducted as follows: (i) we identified the locations of candidate QDs from RtoL images such as Fig. 3(c), (ii) we positioned the STM tip over QDs and measured BEEM  $I_C-V_T$  curves with  $V_R=0$  V and  $V_R=1$  V, (iii) for comparison, we made the same measurements at

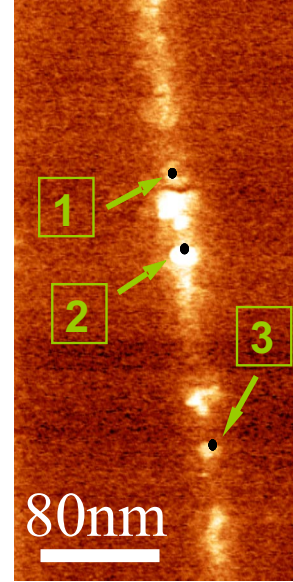


FIG. 7. (Color online) Interleaved RtoL BEEM image of a portion of QD layer No. 2 measured with  $V_T=0.80$  V. The marks show the positions where BEEM spectra were measured.

specific locations in the surrounding GaAs QW region, away from the InGaAs wetting layer. A “set” of ten  $I-V$ 's was measured at a particular location, averaged together to reduce noise, and fit with the BK model to determine the local SBH. The fitting range used to extract the SBH was from 0.5 to 1.05 eV for the data taken away from the QDs. We selected this fitting range in order to avoid the second threshold of  $\sim 1.2$  eV corresponding to the L point of the GaAs conduction band.<sup>17</sup> The fitting range used to extract the SBH was from 0.5 to 0.9 eV for the data taken over the QDs. The arrows in Fig. 7 show three QD locations where BEEM spectra were measured. Figure 8(a) shows typical measured BEEM  $I_C-V_T$  curves away from the QDs over a GaAs region for  $V_R=0$  V (blue data points) and  $V_R=1$  V (red data points) while Fig. 8(b) shows corresponding curves measured over QD No. 1 in Fig. 7. When the tip is over the GaAs the applied reverse bias caused less than a 5 meV change in threshold voltage and almost no change in BEEM current amplitude when  $V_R$  was increased from 0 to 1 V. In contrast, when the tip is over a QD [Fig. 8(b)], we observe a significant reduction  $\sim 50$  meV in threshold voltage and a marked increase in amplitude. Away from the QDs, the average value of the SBH at  $V_R \cong 0$  V bias was  $0.913 \pm 0.002$  eV while the average value of the SBH at  $V_R \cong 1$  V at the same locations was  $0.911 \pm 0.004$  eV. These values were based on a total of 150  $I_C-V_T$  curves taken at five different locations, first measured at  $V_R=0$  V and then repeated at 1 V, with all stated uncertainties determined from statistical fluctuations of repeated measurements at the same tip location. These measurements indicate that away from the QDs the SBH at 1 V is lower by only  $\sim 2 \pm 4$  meV as compared to the SBH at 0 V, roughly consistent with that expected from image force lowering.

Over the three separate QDs indicated in Fig. 7, the measured SBHs for  $V_R=0$  V were 0.778 eV, 0.807 eV, and 0.798 eV, respectively, with a typical statistical uncertainty of 4

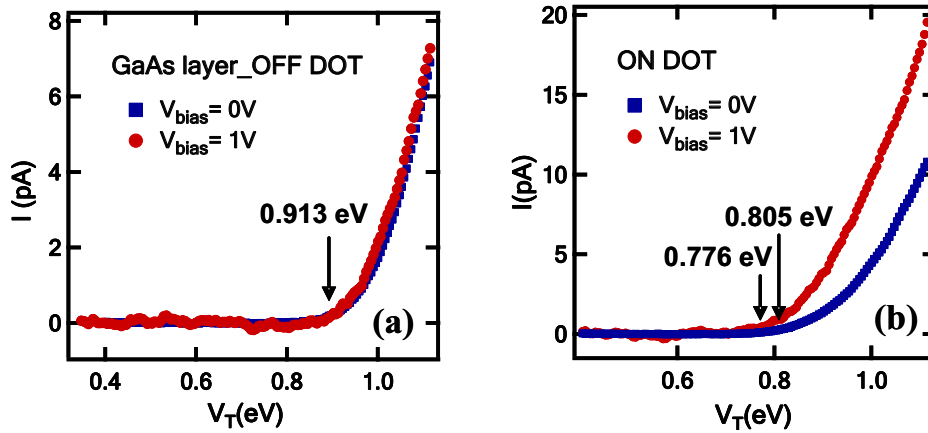


FIG. 8. (Color online) (a) Averaged BEEM spectra over GaAs regions away from the QDs at 0 V bias (square) and 1 V reverse bias (circle). (b) Averaged BEEM spectra taken over InGaAs No. 1 at 0 V bias (square) and 1 V reverse bias (circle).

meV while the measured SBHs at the same locations for  $V_R=1$  V were 0.739 eV, 0.776 eV, and 0.750 eV, respectively, with a typical uncertainty of 14 meV. All three dots had significantly reduced SBHs when  $V_R$  was increased to 1 V, with the reduction ranging from  $\sim 30$  to 50 meV.

These measurements indicate that all three QDs fall under Case B as defined above, with the high point in the CB profile occurring at the back side of the QD. This has several consequences on our interpretation of the data. First, it indicates that when the tip is over a QD, the measured SBH represents the CBM energy of the wetting layer immediately *behind* the QD and not to the CBM of the QD itself. Hence, the relatively low SBHs of 0.78–0.80 eV measured over the QDs are *larger* than the actual CB energy in the dots. Second, it indicates that we should be able to use Eq. (2) above to estimate  $d$ , which is the physical depth of the dots. Using Eq. (2), dots No. 1, 2, and 3 in Fig. 3(c) were found to have physical depths of  $\sim 6$  nm,  $\sim 6$  nm, and  $\sim 9$  nm, respectively. Based on transmission electron microscope (TEM) images such as shown in Fig. 9, we know that the typical width of the QDs in layer No. 2 during growth is about 10 nm, and so the expected depth of a cleaved QD (in the direction perpendicular to the cleaved surface) should be in the range of 0–10 nm. We see that the measured physical depths of the cleaved QDs are consistent with the expected value.

In addition to the significant reduction in the SBH with a 1 V reverse bias when the tip was over a QD, we again note that the BEEM current amplitude was also substantially enhanced over the QD while the reverse bias had little effect on either the BEEM current amplitude or SBH when the tip was over the GaAs region away from the QDs. While we do not yet

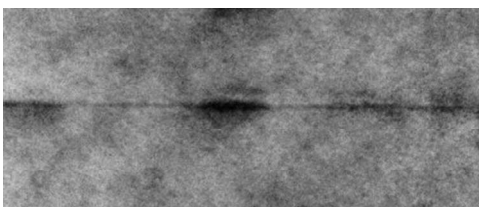


FIG. 9. Transmission electron microscope image of cleaved QD layer No. 2.

have a detailed model to explain why the BEEM current should be so strongly enhanced by the applied reverse bias when the tip is over a QD, we do note that a reverse bias will lower the conduction band in the semiconductor and hence make available extra states for inelastic scattering of injected hot electrons. When the tip is away from the QDs, the high point in the conduction band profile is located very close to the metal interface (as discussed above) so almost all of these extra states will be located deeper in the GaAs than this high point. In this case the extra states would not significantly increase the probability of collecting the injected hot electrons since almost all electrons that travel beyond the high point would have been swept into the substrate by the depletion field and collected anyway. However, when the tip is located over a QD, the high point is located substantially deeper into the substrate ( $\sim 6$ – $9$  nm by the above estimates), so the extra states resulting from the applied bias would enhance inelastic scattering of electrons to the bottom of the QD conduction band, where they could be held in metastable QD states and “leak” into the WL and be collected as enhanced BEEM current. Quantitative modeling is still needed to evaluate this proposed enhancement mechanism.

An important finding of our measurements is the determination of the conduction band minimum energy offset between the GaAs and the wetting layer. The measured CBM energy when the tip was located over the wetting layer but *beside* the locations of the QDs (see Fig. 5), was  $\text{CBM}_{\text{beside}} \cong 0.822 \pm 0.012$  eV (these estimates were based on a total of 300  $I_C$ - $V_T$  curves taken at 30 different WL locations) while the measured CBM with the tip over the GaAs region away from the wetting layer is  $0.913 \pm 0.002$  eV. Therefore, the conduction band minimum energy offset between the GaAs and the wetting layer is approximately 90 meV. We note that since the WL is an electron quantum well, then this measured CB offset includes the *quantum confinement energy* of electrons in the WL quantum well.<sup>16</sup>

We also note that if *Fermi-level pinning* at the Au/WL interface is different from the pinning at the Au/GaAs interface, it is possible that this measured CB offset could be shifted slightly from the true value.<sup>21</sup> To confirm that such a

shift is significant, we also estimated this CB offset using a different procedure that should be almost independent of any differences in the Fermi-level pinning at the Au/WL and Au/GaAs interfaces. As described above, when the tip was located over several QDs, we actually measured the CBM of the wetting layer at the *back side* of these QDs and also the approximate depths where these measured “high points” of the CBM profiles were determined. Since we also know the approximate electric field close to the metal interface [from Eq. (1)], we can extrapolate to estimate *what the CBM of the wetting layer at the metal interface would have been if the QDs had not been present*, using the expression:  $\text{CBM}_{\text{extrap}} \cong \text{CBM}_{\text{back}} + (qE_d)d - \Delta\Phi_{IF}$ . Using this procedure, the extrapolated CMB for the three QDs discussed above were found to be 0.817, 0.829, and 0.840 eV. We see that these values are close the average value  $\text{CBM}_{\text{beside}} \cong 0.82$  eV measured when the tip was over the WL.

The correspondence between  $\text{CBM}_{\text{extrap}}$  and  $\text{CBM}_{\text{beside}}$  is significant because  $\text{CBM}_{\text{extrap}}$  was based on measured CBMs where the high point of the CB profile was at a depth of  $\sim 6\text{--}9$  nm from the metal interface while  $\text{CBM}_{\text{beside}}$  was based on measured CBMs where the high point of the CB profile was very close to the metal interface. Since these measured depths (6–9 nm) are significantly larger than the typical 1 nm width of the WL, then the CBM energy at this depth should be only weakly dependent on the narrow (1 nm) strip of interface states along the metal/WL interface. The physics behind this is essentially the Tung effect<sup>22</sup> for a strip of different barrier height. In particular, using Eq. (8) from Ref. 22, which assumes an infinite strip of width  $W$  with a difference in barrier height of  $\Delta\varphi$  compared to the rest of the interface, the change in potential energy at a depth  $z$  directly below the center of the strip is given by

$$\Delta PE \cong \frac{2\Delta\varphi}{\pi} \tan^{-1} \left[ \frac{W/2}{z} \right]. \quad (3)$$

Assuming a wetting layer width of  $W \cong 1$  nm [estimated from the TEM images taken on this sample] and a depth of  $\sim 6\text{--}9$  nm below the metal/WL interface, then the shift in potential at this depth due to the strip of interface states would only be  $\sim (2/\pi)\tan^{-1}(1/14)$ , or at most 5% relative to the shift right at the metal/WL interface. Since  $\text{CBM}_{\text{extrap}}$  and  $\text{CBM}_{\text{beside}}$  are found to be comparable to each other, we can conclude that any difference in interface pinning between the Au/WL and Au/GaAs interfaces does not produce a significant shift in the measured 90 meV CBM offset as compared to the true CBM offset.

As mentioned in the introduction, the QD/wetting layer/GaAs systems have been heavily investigated using optical spectroscopy techniques including photoluminescence (PL). For example, Schmidt *et al.*<sup>23</sup> reported an average difference of  $\sim 80$  meV between the GaAs band-edge transitions and those involving the InAs wetting layer for an InAs QD system at room temperature, and Leon and Fafard<sup>24</sup> reported a difference of  $\sim 130$  meV at 77 K for an  $\text{In}_{0.6}\text{Ga}_{0.4}\text{As}$  QD system. While these offset voltages are similar to the  $\sim 90$  meV average offset measured here by BEEM, it is difficult to directly compare these results, both because the

exact composition and QD density and structure may vary for different samples, and because PL and BEEM probe different processes. In particular, PL measures optical transitions involving *both* CB electrons and valence-band (VB) holes, both of which might have different energies between the GaAs and the WL. These optical transitions could also include *mixed* transitions, for example, between the CB of the WL and the VB of the GaAs. In contrast, BEEM only probes the conduction band, and so can more directly measure the CB offset between GaAs and the WL. BEEM also has  $\sim 10\text{--}20$  nm spatial resolution while PL and most optical techniques usually average over a much larger area.

Finally, we note that in Fig. 2 the third QD layer (counting from the left-hand side of Fig. 2) has *smaller* BEEM current amplitude than either the first or second QD layer, even though it has a significantly thicker layer of deposited  $\text{In}_{0.4}\text{Ga}_{0.6}\text{As}$  (3.00 nm for layer No. 3 vs 2.04 nm for layer No. 2 and 1.56 nm for layer No. 1). We also note analogous behavior for the pure InAs layer No. 5 which has smaller BEEM amplitude than layer Nos. 6 and 7 even though it has a thicker layer of deposited InAs (0.656 nm for layer No. 5 vs 0.596 nm for layer No. 6 and 0.546 nm for layer No. 7). At first glance this is puzzling since we would naively expect that a layer with more deposited In would be physically thicker and/or have a lower SBH and so would have larger BEEM current amplitude.

However, it is known that beyond a deposited layer thickness rapid QD growth depletes In from the WL at a faster rate than it is deposited such that the In content of the WL actually decreases.<sup>13</sup> This would result in a reduced physical thickness and/or reduced concentration in the WL, both of which would suppress the BEEM current amplitude. A reduced WL thickness would reduce the cross-sectional area for hot electrons to enter the WL from the Au film and so would reduce BEEM current.<sup>25</sup> A reduction in BEEM current would also result from an increased SBH, due either to an increased CBM in the InGaAs WL (if the In concentration is reduced) or by increased quantum confinement (if the WL thickness is reduced). Hence the observed reduction in BEEM current in layer No. 3 (compared to layer Nos. 1 and 2) and in layer No. 5 (compared to layer Nos. 6 and 7) can be explained in a natural way by a reduction in In content in the WL due to large-scale QD growth. This directly shows that the WL becomes “electrically thinner” following large-scale QD growth.

#### IV. CONCLUSIONS

In summary, we measured the conduction band minimum energy in the wetting layer around and at the physical depth of cleaved  $\text{In}_{0.4}\text{Ga}_{0.6}\text{As}$  quantum dots using XBEEM. The reduction in the measured barrier height due to the applied reverse bias confirms that XBEEM measured the conduction band minimum energy in the wetting layer at the backside of the quantum dots. We used the measured conduction band minimum energies to estimate the physical depth of the cleaved quantum dots. We found that SBH over the QDs were reduced by  $\sim 30\text{--}50$  meV due to the applied bias, giving an estimated depth  $d \cong 6\text{--}9$  nm of the backside of the

QDs, consistent with the known size of these QDs. We also found an offset of 90 meV between the conduction band minimum energy of the wetting layer and GaAs, including any quantum confinement energy of the electrons in the WL. By comparing the CBM energy in the wetting layer measured beside the QDs to the extrapolated CBM energy based on the measured CBM energy at the back side of the QDs, we conclude that the measured 90 meV offset is not significantly shifted by any differences in Fermi-level pinning at the Au/GaAs and Au/WL interfaces. The amplitude of the BEEM current entering a WL was also observed to *decrease* once the deposited thickness of the  $\text{In}_{0.4}\text{Ga}_{0.6}\text{As}$  or InAs layer exceeded a certain threshold, consistent with a deple-

tion of In from the WL after large-scale QD formation takes place.

#### ACKNOWLEDGMENTS

This work was supported by the National Science Foundation under Grants No. DMR-0505165 and No. DMR-0805237. The authors would like to acknowledge the assistance of Michael Coviello at TEM Analysis, Inc. Sandia is a multiprogram laboratory operated by Sandia Corporation, a Lockheed Martin Co., for the United States Department of Energy's National Nuclear Security Administration under Contract No. DE-AC04-94AL85000.

- 
- <sup>1</sup>P. Michler, A. Kiraz, C. Becher, W. V. Schoenfeld, P. M. Petroff, L. Zhang, E. Hu, and A. Imamoglu, *Science* **290**, 2282 (2000).
- <sup>2</sup>E. Moreau, I. Robert, L. Manin, V. Thierry-Mieg, J. M. Gérard, and I. Abram, *Phys. Rev. Lett.* **87**, 183601 (2001).
- <sup>3</sup>Z. Yuan, B. E. Kardynal, R. M. Stevenson, A. J. Shields, C. J. Lobo, K. Cooper, N. S. Beattie, D. A. Ritchie, and M. Pepper, *Science* **295**, 102 (2002).
- <sup>4</sup>C. Santori, D. Fattal, J. Vučković, G. S. Solomon, and Y. Yamamoto, *Nature (London)* **419**, 594 (2002).
- <sup>5</sup>D. Gammon, E. S. Snow, B. V. Shanabrook, D. S. Katzer, and D. Park, *Science* **273**, 87 (1996).
- <sup>6</sup>P. Borri, W. Langbein, S. Schneider, U. Woggon, R. L. Sellin, D. Ouyang, and D. Bimberg, *Phys. Rev. Lett.* **87**, 157401 (2001).
- <sup>7</sup>M. Bayer and A. Forchel, *Phys. Rev. B* **65**, 041308 (2002).
- <sup>8</sup>D. Bimberg, M. Grundmann, and N. N. Ledentsov, *Quantum dot heterostructure* (Wiley, Chichester, 1999), and references therein.
- <sup>9</sup>I. N. Stranski and L. Krastanow, *Sitzungsber. Akad. Wiss. Wien, Math.-Naturwiss. Kl., Abt. 2B* **146**, 797 (1939).
- <sup>10</sup>Y. Toda, O. Moriwaki, M. Nishioka, and Y. Arakawa, *Phys. Rev. Lett.* **82**, 4114 (1999).
- <sup>11</sup>C. Kammerer, G. Cassaboïs, C. Voisin, C. Delalande, Ph. Rousignol, and J. M. Gérard, *Phys. Rev. Lett.* **87**, 207401 (2001).
- <sup>12</sup>F. A. Vasanelli, R. Ferreira, and G. Bastard, *Phys. Rev. Lett.* **89**, 216804 (2002).
- <sup>13</sup>J. G. Cederberg, *J. Cryst. Growth* **307**, 44 (2007).
- <sup>14</sup>J. G. Cederberg, F. H. Katz, and R. M. Biefeld, *J. Cryst. Growth* **261**, 197 (2004).
- <sup>15</sup>Q. Xie, A. Madhukar, P. Chen, and N. P. Kobayashi, *Phys. Rev. Lett.* **75**, 2542 (1995).
- <sup>16</sup>C. Tivarus, J. P. Pelz, M. K. Hudait, and S. A. Ringel, *Phys. Rev. Lett.* **94**, 206803 (2005).
- <sup>17</sup>W. J. Kaiser and L. D. Bell, *Phys. Rev. Lett.* **60**, 1406 (1988); L. D. Bell and W. J. Kaiser, *ibid.* **61**, 2368 (1988).
- <sup>18</sup>S. M. Sze, *Physics of Semiconductor Devices*, 2nd ed. (Wiley, New York, 1981).
- <sup>19</sup>L. D. Bell, S. J. Manion, M. H. Hecht, W. J. Kaiser, R. W. Fathauer, and A. M. Milliken, *Phys. Rev. B* **48**, 5712 (1993).
- <sup>20</sup>M. H. Hecht, L. D. Bell, and W. J. Kaiser, *Appl. Phys. Lett.* **55**, 780 (1989).
- <sup>21</sup>C. Tivarus, K.-B. Park, M. K. Hudait, S. A. Ringel, and J. P. Pelz, in *Characterization and Metrology for ULSI Technology 2005*, edited by D. G. Seiler, A. C. Diebold, R. McDonald, C. R. Ayre, R. P. Khosla, S. Zollner, and E. M. Secula (American Institute of Physics, New York, NY, 2005), p. 280.
- <sup>22</sup>R. T. Tung, *Phys. Rev. B* **45**, 13509 (1992).
- <sup>23</sup>K. H. Schmidt, G. Medeiros-Ribeiro, J. Garcia, and P. M. Petroff, *Appl. Phys. Lett.* **70**, 1727 (1997).
- <sup>24</sup>R. Leon and S. Fafard, *Phys. Rev. B* **58**, R1726 (1998).
- <sup>25</sup>C. Tivarus, J. P. Pelz, M. K. Hudait, and S. A. Ringel, *Appl. Phys. Lett.* **87**, 182105 (2005).